Research Article | Vol. 28, No. 24 / 23 November 2020 / Optics Express 36822
Optics EXPRESS

Halo effect in high-dynamic-range mini-LED backlit LCDs

EN-LIN HSIANG, QIAN YANG, ZIQIAN HE, JUNYU ZOU, AND SHIN-TSON WU*

College of Optics and Photonics, University of Central Florida, Orlando, Florida 32816, USA
**swu@creol.ucf.edu*

Abstract: We develop an optical model including the glare effect in the human vision system to analyze the halo effect of high-dynamic-range (HDR) mini-LED backlit liquid crystal displays (LCDs). In our model, an objective function is first introduced to evaluate the severity of the halo effect with different image contents. This function is further combined with PSNR to establish a new evaluation metric to analyze the image quality affected by the halo effect. A subjective visual experiment is also conducted to verify the above-mentioned evaluation metrics. In addition, we analyze the influence of ambient environment (viewing angle and ambient light illuminance) on the halo effect. After considering the requirements on local dimming zones, dynamic contrast ratio, gamma shift, and color shift for practical applications, we find that fringe-field-switching mode is a strong contender for the mini-LED backlit LCD system.

1. Introduction

High dynamic range (HDR) is a key requirement for next-generation display technologies [1,2]. To achieve HDR, three criteria should be satisfied: 1) True black state and high peak brightness, namely high contrast ratio (CR>10^5:1), 2) wide color gamut (≈90% BT2020), and 3) more than 10-bit (1024) gray levels [3–5]. These demands are still challenging for presently dominating liquid crystal displays (LCDs) and organic light-emitting diode (OLED) displays [6]. The contrast ratio of an LCD is limited by the depolarization effects from thin-film-transistor array, LC layer, and color filters, and it also depends on the LCD mode employed. For multi-domain vertical alignment (MVA) LCD, its CR≈5000:1, while for fringe-field-switching (FFS) LCD its CR ≈2500:1 [7,8]. Although OLED exhibits an unprecedented contrast ratio (CR≈10^6:1), its peak brightness and lifetime remain to be improved [9].

To enhance an LCD's contrast ratio, the dark state light leakage should be suppressed. Local dimming is an effective technique for improving the dynamic contrast ratio [10–13], and it has been employed in both direct-lit and edge-lit LCDs [14–16]. The edge-lit configuration offers a thinner profile which is desirable for mobile displays, but its HDR performance is limited by the small number of local dimming zones. On the other hand, the direct-lit approach can achieve a much higher CR, but the tradeoff is increased panel thickness. Recently, with the rapid development of mini-LED (chip size: 100-500 μm) backlight, both HDR and thin profile can be achieved [17–20]. The backlight unit is divided into hundreds to thousands of locally dimmable zones, and each zone can independently adjust the illuminance according to the image contents. In the dark image areas, the corresponding mini-LED zones can be dimmed locally, while in the bright areas the backlight can be boosted accordingly. Thus, the dynamic CR of the LCD can be significantly improved. However, a disadvantage of local dimming technique is the halo effect [21,22]. Halo artifacts usually appear at the edges of bright objects surrounded by dark background. In the edge area, the backlight segment is turned on to provide a sufficient illumination for the bright objects. As a result, the luminance of dark background surrounding the bright objects depends on the LCD's native contrast ratio, which is ~2500:1 (FFS-LCD). On the other hand, the mini-LED backlight is turned off in the areas far away from bright objects to

#413133 https://doi.org/10.1364/OE.413133
Journal © 2020 Received 23 Oct 2020; revised 12 Nov 2020; accepted 12 Nov 2020; published 18 Nov 2020

Optics EXPRESS

show the true dark state. Therefore, the relatively high brightness at the edges of bright objects can cause halo artifacts. Many backlight dimming algorithms [23–26] have been proposed to reduce the halo effect. According to [27], the halo effect can be reduced by increasing the LCD's native contrast ratio and the number of local dimming zones. However, there are still several unanswered questions regarding the halo effect in mini-LED backlit LCDs (abbreviated as mLCDs). For instances, 1) when a display image received by the human vision system (HVS) [28,29], the light scattering (glare spread function) inside human eye would spread out the light intensity from bright areas, thereby smearing the halo artifacts. 2) Whether the halo effect is noticeable depends heavily on the image content itself, but for a long time, there has been lacking objective methods to evaluate the difficulty of how HVS can observe halo effect in an image. 3) How does the viewing environment, such as viewing angle and ambient light intensity, affect the halo effect?

In this paper, we develop an optical model to simulate the images produced by an HDR mLCD, and then based on the CIE standard glare spread function [30] we obtain the retinal image received by HVS. The influence of glare effect on halo artifacts in HVS is analyzed. In addition, to determine the difficulty for HVS to observe the halo effect in an image, an objective evaluation function called D-value is proposed and verified by subjective experiments. Unlike most evaluation metrics that usually consider the entire image content, the evaluation metric LocalPSNR defined as PSNR (peak signal-to-noise ratio) in a local area with a larger D-value is proposed to reflect the degraded image quality from halo effect. In practical applications, the influence from ambient environment, such as viewing angle and ambient light illuminance, is very important. As the ambient light increases, the surface reflection could washout the halo artifacts, and as the viewing angle increases which leads to an increased light leakage, the requirement of local dimming zone becomes stricter. Through our analysis, FFS mode offers several attractive features for the mLCD system.

2. Device modeling

2.1. Displayed image simulation: human vision system

In an mLCD system, the light emitted from mini-LED chips is modulated by some optical films, such as quantum dot enhancement film, optical diffuser, and brightness enhancement film, before reaching the LC panel. Therefore, the light intensity distribution is highly related to the optical design in the backlight unit. Here, we simulate a 15.6-inch 3840×2160 LCD with a mini-LED backlight unit composed of 20,736 (108×192) LED chips with a pitch of 1.8 mm. According to [22], we use following Gaussian function to present the light profile of a single mini-LED:

$$I(x_{LED}) \propto \exp - \left[\frac{(x_{LED} - x_{LED\_c})^2}{2\sigma^2} \right], \tag{1}$$

where x_{LED_c} is the locus of the mini-LED and σ is an expansion characteristic parameter. In our simulation, the ratio of σ to the mini-LED pitch is 0.6, which provides the backlight with a uniformity larger than 97%. Figure 1 illustrates the simulation process based on the point spread function theory [31] for generating HDR mLCD images. In this example, the LCD panel has a CR = 5000:1 and there are 162 local dimming zones in the backlight unit; each zone contains 12×12 mini-LEDs. First, the image is divided into several segments according to the number of local dimming zones. The mini-LED brightness in each zone depends on the maximum brightness in that zone, as shown in Fig. 1(a). Next, we apply the point spread function to each zone to calculate the luminance distribution on the LC layer in Fig. 1(b). After that, an 8-bit LC panel is used to modulate the luminance of each sub-pixel to achieve the target image content as Fig. 1(c) shows. To illustrate the halo effect more clearly, we depict the normalized contrast ratio

Optics EXPRESS

distribution (the brightness of each pixel divided by the peak brightness of the display image) in Fig. 1(d), where the halo artifacts surrounding the chess crown are displayed.

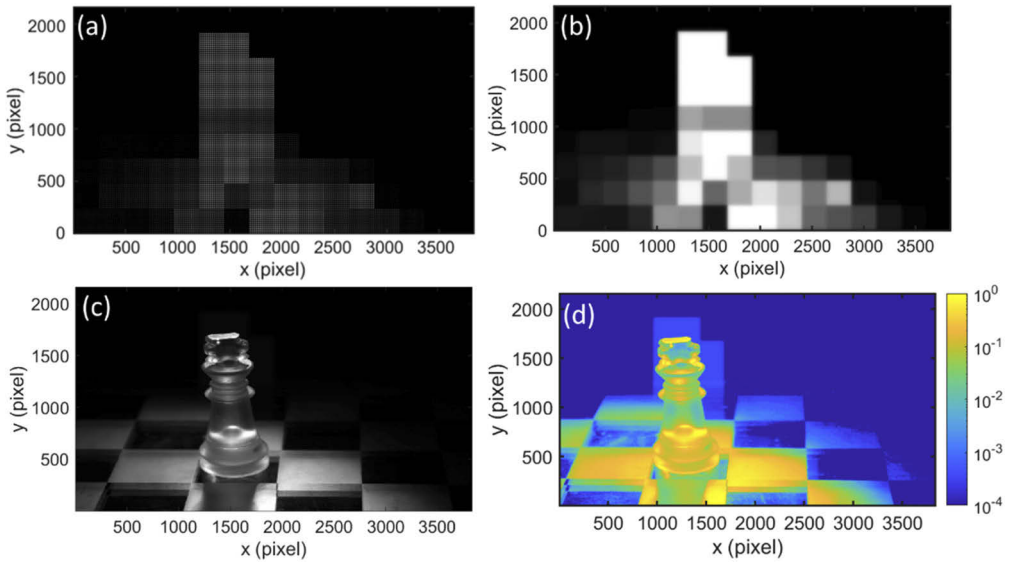

Fig. 1. Displayed image of a mLCD: (a) Intensity profile of the mini-LED backlight. (b) Luminance distribution of the light incident on LC layer. (c) Displayed image after LCD modulation. (d) Normalized contrast ratio distribution of the image displayed by mLCD.

So far, we have successfully simulated the image performed by HDR mLCD and clearly observed the halo effect in the simulated image. However, the observer receives all the displayed images through eyes. Therefore, considering the light scattering in human eye, known as *glare*, is very important to accurately analyze the halo artifacts received by the HVS. Here, we call the image on the display panel as "display image", and that received by the observer through HVS as "retinal image". According to the scattered light of human eye, one pixel will spread the light to adjacent pixel, and at the same time, the light from adjacent pixel will also be scattered to the pixel. To analyze the glare effect of human eye, the glare spread function from the CIE standard [30] is described below to simulate the relative light intensity scattered from one pixel to another:

$$\begin{aligned} Relative\_Luminance &= [1 - 0.08 \times (\tfrac{Age}{70})^4] \times \left[\frac{9.2\times10^6}{\left[1+(\frac{\theta}{0.046})^2\right]^{1.5}} + \frac{1.5\times10^5}{\left[1+(\frac{\theta}{0.045})^2\right]^{1.5}} \right] \\ &+[1 + 1.6 \times (\tfrac{Age}{70})^4] \times \left\{ \left[\frac{400}{1+(\frac{\theta}{0.1})^2} + 3 \times 10^{-8} \times \theta^2 \right] + p \times \left[\frac{1300}{[1+(\frac{\theta}{0.1})^2]^{1.5}} + \frac{0.8}{[1+(\frac{\theta}{0.1})^2]^{0.5}} \right] \right\} + 2.5 \times 10^{-3} \times p, \end{aligned} \tag{2}$$

where θ is the visual angle between emitting and receiving pixels, *Age* stands for the observer's age, and p is the observer's pigmentation. To be consistent with our subjective experiment, here we set $p = 0$ (dark eyes) and $age = 25$.

According to the visual angle between each pixel, the normalized glare spread function under 550-mm viewing distance is plotted in Fig. 2(a). Employing the glare spread function to "display image", we simulate the contrast ratio distribution in "retinal image", as shown in Fig. 2(b), including the influence of light scattering from human eye. Since light scattering occurs inside human eye, the light from high brightness pixels will spread to neighboring pixels, which smears the local contrast. As a result, the halo artifacts become blurred and are difficult to distinguish.

A simple image content consisting of a white dot surrounded by a dark background is used to further analyze the influence of glare effects on halo artifacts. Figure 3(a) depicts the contrast

Optics EXPRESS

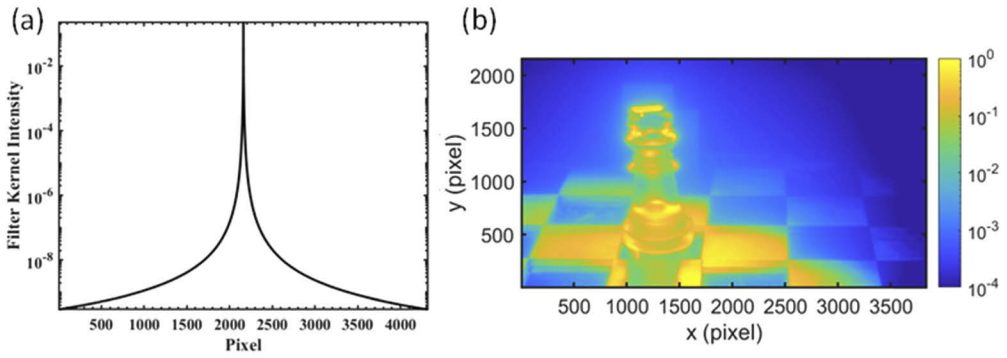

Fig. 2. (a) The CIE standard glare spread function under the viewing condition in our subjective experiments. (b) Simulated retinal contrast ratio distribution.

ratio distribution of the display image generated by an HDR mLCD with CR = 5,000:1 and an OLED display with CR = 1,000,000:1. The number of local dimming zone ranges from 18 to over 20,000. As shown in Fig. 3(a), even if the number of local dimming zones exceeds 20,000, we can still easily identify the brightness difference on the area adjacent to the central white point. However, if the glare effect is taken into consideration, the light from central white point will be scattered to adjacent pixels, as Fig. 3(b) shows. Here, we refer to the image blur produced by the HVS as eye-halo. As the number of local dimming zones increases, the effect of eye-halo gradually dominates so that it is difficult to distinguish the halo artifacts produced by mLCD. This glare effect of HVS explains why an HDR mLCD can exhibit comparable image quality as an OLED display. However, based on the image contrast ratio distribution alone is difficult to distinguish the limitation of HVS. Therefore, in Section 3 we conduct subjective experiments to define the perception limits of the test images.

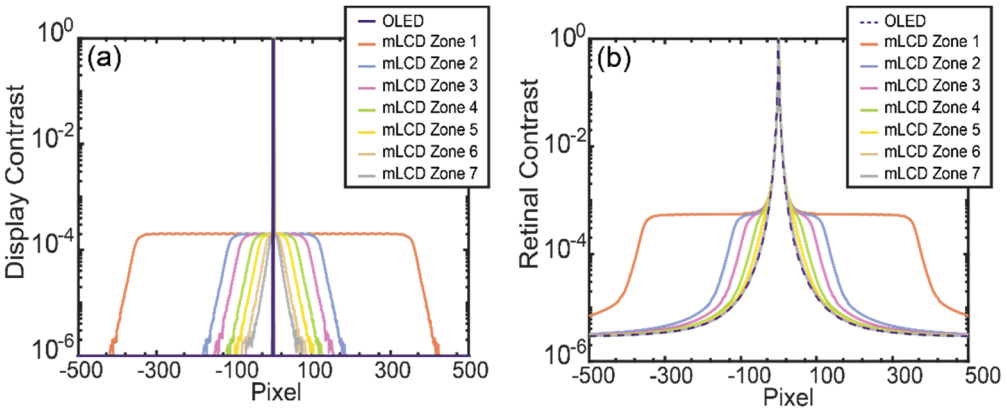

Fig. 3. Comparison of image contrast between mLCD and OLED display: (a) Display image, and (b) retinal image (glare effect). The number of local dimming zones corresponding to Zone 1 to 7 is 18, 162, 288, 648, 1458, 5832, and 23328, respectively.

2.2. Halo effect evaluation metrics: D-value and local PSNR

As mentioned above, whether the halo effect is noticeable to HVS depends largely on the image content itself. Therefore, to suppress the halo effect, the required local dimming zone number will vary for different image contents. As described in [16], the number of local dimming zones

Optics EXPRESS

differs by nearly two orders of magnitude among the images investigated. For a long time, there was no objective method to evaluate such phenomenon. To overcome this problem, we use two factors to evaluate how HVS can observe halo effect in an image: 1) Local contrast ratio. When the local contrast ratio is high, to maintain the local high brightness the backlight should be bright. As a result, the halo effect in the dark area is more serious. 2) Local average luminance. The JND (just noticeable difference) of the human visual system is related to the average brightness [32]. When the local average brightness is low, the JND is also low, so the halo effect can be observed more easily. Therefore, here we propose a new evaluation method called "D-value", which is the ratio of local contrast to local average brightness in an image, to assess the difficulty for the HVS to observe halo effect. The D-value can be defined as:

$$D-value = \frac{Local\ contrast\ ratio}{Local\ average\ brightness} = \frac{\left[\frac{Max(I(i,j))}{Min(I(i,j))}\right]_{\substack{i\in(1,M)\\ j\in(1,N)}}}{\left[\frac{1}{M\times N}\sum_{i=1}^{M}\sum_{i=1}^{N} I(i,j)\right]}, \tag{3}$$

where M and N represent the numbers of pixels in the local area. In the following, we will explain how to define the size of a local area. Based on HVS, when the eccentric angle increases, human vision will be greatly reduced. Foveal vision corresponding to high-resolution areas is usually defined as $< \pm 2.0°$ from the center of fovea [33]. Therefore, we define the size of the local area corresponding to an eccentric angle $\pm 1.2°$. Under our subjective experiment setting, the angle range ($\pm 1.2°$) represents the surface area of 240 pixels × 240 pixels on the display panel. According to the number of local dimming zones, a local area may contain different numbers of local dimming zones. For example, the 4K2 K display panel is divided into 162 local areas according to the local area size. When the number of local dimming zones is 162, 648 or 1458, one local area contains 1, 4, or 9 local dimming zones, respectively. In addition, the location of local area is aligned with the local dimming zones of the mini-LED backlight, as shown in Fig. 4. For the local area, the border is drawn in red, and for the local dimming zones, the border is drawn in black. According to the number of local dimming zones, the outer boundary of local area corresponds to 1, 4 or 9 local dimming zones.

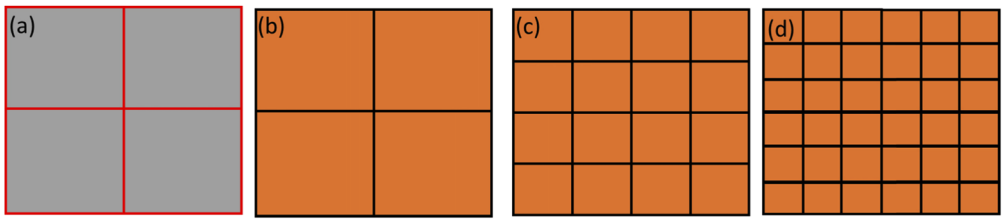

Fig. 4. The relative position of (a) local area and local dimming zones with (b) 162, (c) 648, and (d) 1458 zones.

The test image shown in Fig. 5(a) is used to illustrate how we define the local area and calculate the corresponding D-value. First, we down sample the image according to the local area size (162 local areas). Because one local area may contain more than one local dimming zones, the brightness of the local area is determined by the maximum brightness of the local dimming zones inside the local area, as shown in Fig. 5(b). As mentioned above, halo artifacts usually appear on the edges of bright objects surrounded by dark backgrounds. Therefore, there are two conditions for the halo artifacts to appear in local areas: 1) in the local area, any local dimming zone is in a high brightness state, and 2) the local dimming zone of the adjacent local area is turned off, i.e. dark background. In order to find local areas that may have halo artifacts, we first find local areas with gray levels greater than 150 (bright objects). After that, 8 adjacent local areas surrounding the bright local areas are evaluated. If there are more than 3 adjacent areas with gray levels below

Optics EXPRESS

150, we say that the bright local area is surrounded by a darker background. Finally, we find the edge where the brightness changes sharply, as shown in Fig. 5(c). In Fig. 5(d), we have outlined five local areas, where the highest D-values are represented by red lines, and their corresponding D-values are listed inside the boxes. In Fig. 5(d), based on the D-value method, we predict the local areas with a larger D value should have more severe halo artifacts. If we compare the local areas plotted in Fig. 5(d) with halo artifacts shown in Fig. 1(d), the plotted local area has a good match with the region where halo artifacts occur. Therefore, we verify that our D-value method can reflect where the halo artifacts occur.

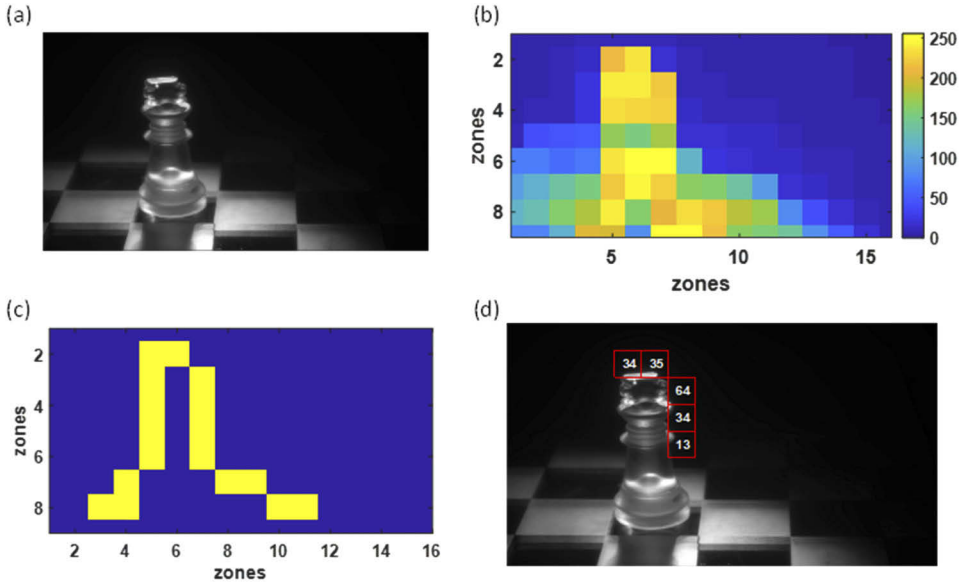

Fig. 5. (a) The test image; (b) The down sampled image according to HVS; (c) The local area may have halo artifacts; (d) The top five D-values in the local area may have halo artifacts.

By applying the D-value evaluation method to a target image, the local area where the HVS is easier to detect the halo artifacts is found. To quantitatively analyze the halo effect in these local areas, an evaluation metric called peak signal-to-noise ratio (PSNR) is applied. Here, the PSNR in these local areas is called LocalPSNR, which is defined as:

$$LocalPSNR = 10 \times \log_{10}\left[\frac{(I_{\max})^2}{\frac{1}{M\times N}\sum_{i=1}^{M}\sum_{j=1}^{N}(\Delta I(i,j)^2)}\right], \tag{4}$$

where M and N represent the number of pixels in the local area (240×240), I_{max} is the difference between black and white, and ΔI is the brightness difference between simulated retinal image and target retinal image. Unlike the PSNR of an entire image that considers all pixels in the image, the advantage of LocalPSNR is that we can exclude pixels that are far away from areas where halo artifacts occur. Taking the 4K2 K images as an example, there are approximately 8-million pixels in each image. However, only pixels at the edge of bright objects surrounded by a dark background will be affected by the halo artifacts. Therefore, compared to the PSNR of entire image, LocalPSNR can reflect the degraded image quality by halo effect more accurately. Let us take the test image shown in Fig. 5(a) as an example.

Optics EXPRESS

Through the model described in Section 2.1, we simulated the retinal image of a mLCD system with seven different local dimming zone numbers (18, 162, 648, 1458, 5832, and 23328) and four LC contrast ratios (1000:1, 1588:1, 2500:1 and 5000:1). To further explain the function of LocalPSNR, we plot the normalized contrast ratio distribution of OLED display in Fig. 6(a), and mLCD system with 162 and 648 local dimming zones in Figs. 6(b) and 6(c) for comparison. The boundary of local areas defined by the D-value method is outlined by red color. First, we can clearly observe that as the number of local dimming zones increases, the halo artifacts inside the local area decreases. Therefore, the image of mLCD inside the local areas becomes more comparable to that of OLED display. This image quality improvement is also reflected by the higher LocalPSNR in Fig. 6(d). As a result, for discussing the image quality degradation results from the halo artifacts, we think analyzing the image quality inside these local areas is convincing and more efficient. The LocalPSNR of all simulated images are calculated and shown in Fig. 6(d). In line with our expectation, a higher contrast ratio and more local dimming zones help eliminate halo artifacts, thereby improving the image quality of the mLCD.

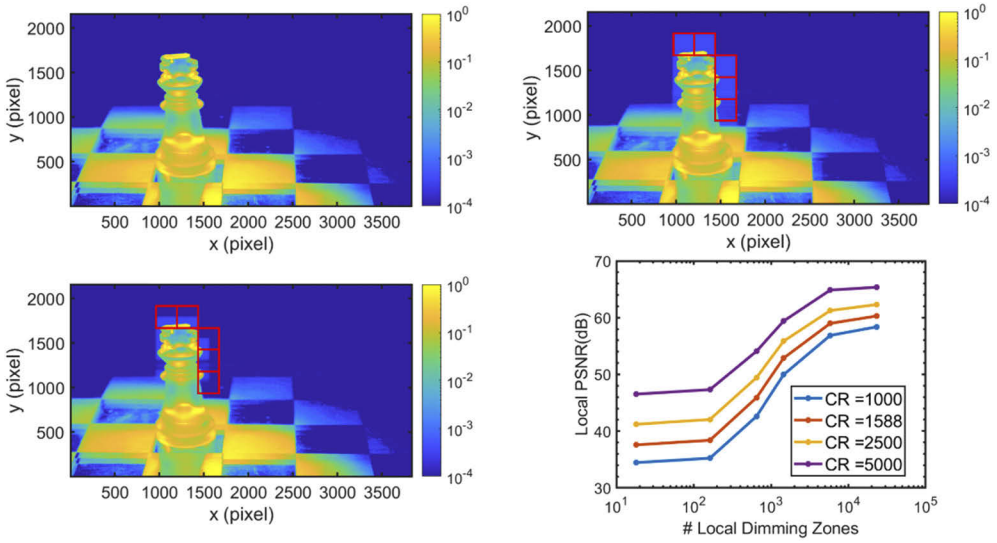

Fig. 6. Normalized contrast ratio distribution of the image generated by (a) OLED display, (b) mLCD with 162 local dimming zones, and (c) mLCD with 648 local dimming zones. (d) Simulated LocalPSNR of target images.

2.3. *Viewing environment effect*

In the above discussion, the viewing environment is completely dark, and the viewing angle is in the normal direction. However, in practical applications, the viewing environment has a significant impact on the halo effect of mLCD. When displaying images under ambient light conditions, the total brightness received by the human eye consists of two parts: displayed signal and ambient light reflected from the display surface [34]. Here, we conduct an experiment to measure the ambient light reflected from the display (OLED laptop Dell XPS15) as shown in Figs. 7(a) and 7(b). Two floor lamps and two ceiling lamps were used to generate four levels of ambient lighting conditions, namely 0 lux, 100 lux, 300 lux and 500 lux. The corresponding reflected ambient luminance measured by the luminance meter was 0 nit (below the measurement capability), 0.46 nit, 1.26 nit, and 2.47 nit, respectively. The corresponding surface reflectivity is about 1.5%. A simple image with a white dot in the center and surrounded by dark background was used to analyze the ambient light effect on halo artifacts. Through adding the reflected

Optics EXPRESS

ambient luminance to the displayed image and including the glare effect of HVS, the retinal image comparison between the OLED display and the mLED (162 zones) is shown in Fig. 8(a). In addition, in Fig. 8(b) we also plot the comparison with 4% surface reflectivity, which is the normal value for commercial touch panels.

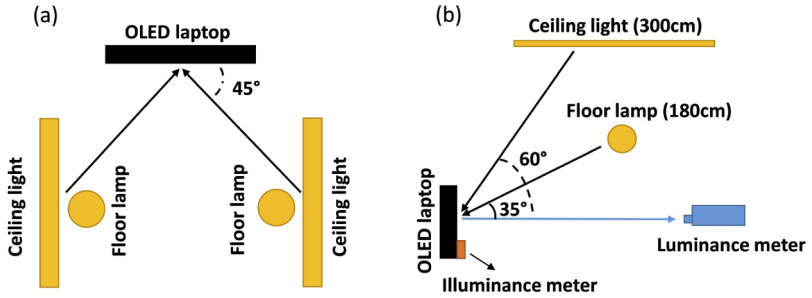

Fig. 7. (a) The ambient light source arrangement (bird view) and (b) measurement condition (side view) in the ambient light experiment.

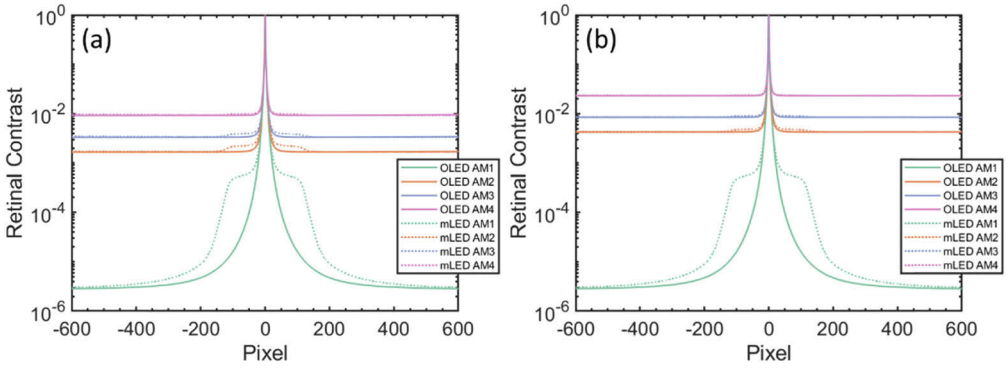

Fig. 8. The contrast ratio of retinal image generated by an OLED display and a mLCD under different ambient illuminances and surface reflectivity (a) 1.5%, and (b) 4%. The ambient (AM) 1 to 4 corresponds to 0 lux, 50 lux, 100 lux, and 300 lux, respectively. The peak brightness of mLCD and OLED display is 400 nits.

We can clearly observe that the halo artifacts in the adjacent areas of the central bright spot are washed out by the reflected ambient light. As a result, as the ambient light brightness increases, the number of local dimming zones required for an mLCD to maintain the same image quality as an OLED display decreases. The subjective experiments in the following section will further verify this phenomenon.

3. Subjective experiment

3.1. Experimental setup

Based on the optical simulation process described above, a quantity D-value is proposed to evaluate the difficulty of HVS to distinguish halo effect with various image contents. After that, LocalPSNR is applied to reflect the local area image quality where the halo artifacts appear. However, it is necessary to further define the minimum LocalPSNR value (perceptual limit) so that HVS cannot distinguish the halo artifacts in an mLCD. In addition, by adding reflected ambient light to the displayed image, we find that the halo artifacts could be washed out by

Optics EXPRESS

the ambient light. However, perception limit in various ambient conditions is still unknown. Therefore, in this section, a subjective experiment is designed to find the perceptual limit of each image. The local dimming zone number required to display images with indistinguishable halo effects under different image contents and different ambient light conditions is obtained.

As shown in Fig. 9, five images are used in our subjective experiment. To choose a proper test image, several factors should be considered, depending on the objectives. In this paper, our purpose is to analyze the halo artifacts in an HDR mLCD. Therefore, all the selected test images exhibit a high contrast ratio, including high peak brightness and good dark state. In addition, the distribution of dark and bright objects also affects the halo artifacts. Normally the image with small bright spots (high spatial frequency components) may have more severe halo artifacts [27]. Therefore, in our test images shown in Fig. 9(a) and Fig. 9(e), small bright spots are scattered in the dark background, while in Fig. 9(c) the bright and dark areas are clearly separated. Figures 9(b) and 9(d) are in the middle of two extreme conditions. Ten people with normal or corrected vision participated in the subjective experiment. Half of them are display experts with basic knowledge of halo effect, and the rest are ordinary people without relevant knowledge. Four different ambient light illuminances are used to study the impact of ambient lighting. The ambient light setting is the same as Fig. 7(a), and the background behind the monitors is a white painted wall. One thing that should be mentioned is that the floor lamp is on the left and right behind the observer, so there is no direct light from the illuminator to the observer. Two OLED panels (Dell XPS 15 laptop, panel size 15.6-inch, resolution 3840×2160) are employed as the image sources and placed 55-cm away from the observer. One of the OLED panels displays a simulated image of mLCD with different local dimming zone numbers and contrast ratios. The other OLED panel displays the control image. Observers are asked to determine whether they can find the difference (halo artifacts) between a pair of displayed images. In one test image, 112 pairs (7 different numbers of local dimming zones, 4 different ambient light illuminances, 4 different LCD contrasts) of images are displayed to each observer. In order to avoid the effects of visual fatigue and prejudice, the observers are required to close their eyes between each pair of images, and the simulated image and the control image will be randomly displayed on one of the laptops. In addition, the interval between each ambient light is 15 minutes to ensure correct visual adaptation.

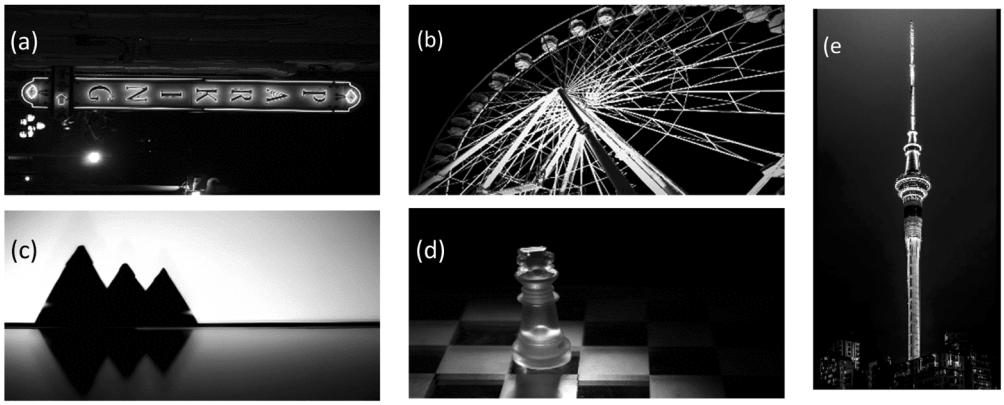

Fig. 9. HDR target images for the subjective experiments: (a) Parking sign, (b) Ferris wheel, (c) Mountains, (d) Chess, and (e) Tower.

Optics EXPRESS

3.2. Perception limits

Based on the method described above, the LocalPSNR values of all test images under dark room condition are shown in Fig. 10. The experiment data from human vision test is plotted as a function of LocalPSNR values in Fig. 11.

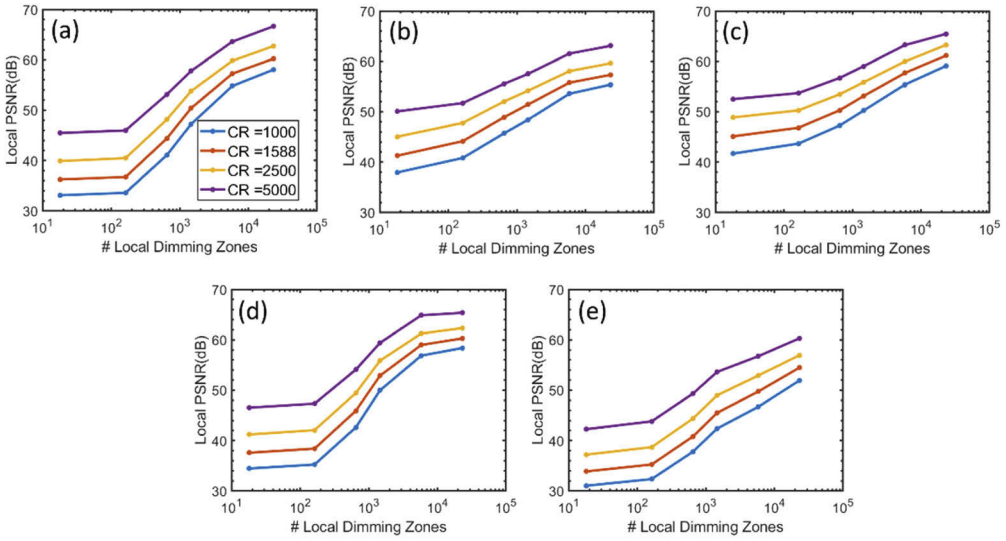

Fig. 10. Simulated LocalPSNR of target images under dark room: (a) Parking sign, (b) Ferris Wheel, (c) Mountains, (d) Chess, and (e) Tower.

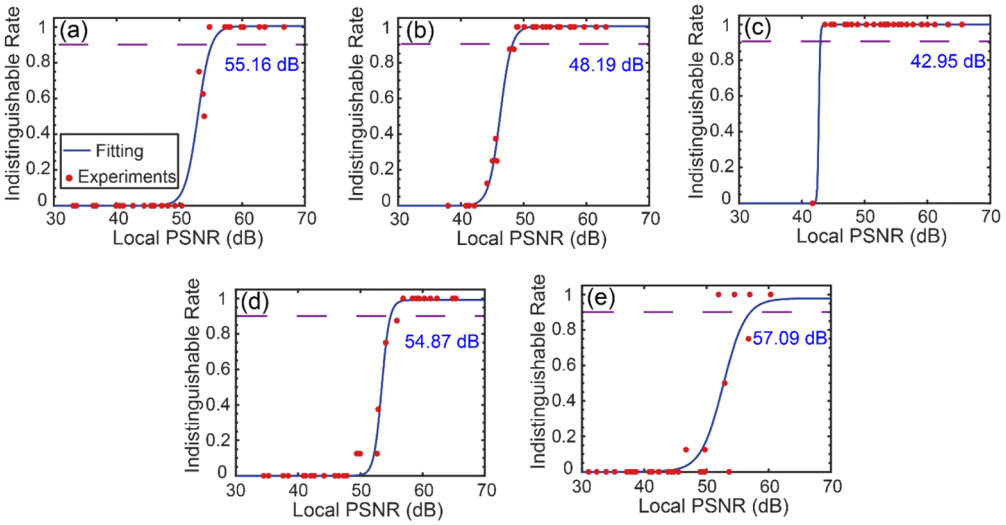

Fig. 11. Measured perception limit of target images under dark room: (a) Parking sign, (b) Ferris Wheel, (c) Mountains, (d) Chess, and (e) Tower.

In Fig. 11, the indistinguishable rate is the ratio of participants who cannot distinguish the target images from the simulated displayed images by the mLCD system. Under certain ambient light condition, for one target image, the local PSNR value varies in a large range due to different contrast ratio and number of local dimming zones. We assume that the observers

Optics EXPRESS

cannot distinguish rendered image and target image when the local PSNR value is above a critical value, called perception limit. It is worth mentioning that the perception limit could vary among different viewers, so the perception limit should be derived using statistical method. To illustrate how the perception limit is found, let us take the chess in Fig. 9(d) as an example. The experimental results of human vision test on chess figure with no ambient light are show in Fig. 11(d). The indistinguishable rate is between 0 and 1. On one hand, when the local PSNR value is small, almost all observers can distinguish these two images, resulting in zero indistinguishable rate accumulated in that region. On the other hand, indistinguishable rates saturate to one at high local PSNR values. The perception limit should locate at somewhere in between these two regions. The scattering plot of the experimental data suggests a logistic function could be used in the curve fitting. In our fitting, the indistinguishable rate (f) follows:

$$f(x) = \frac{1}{1 + \exp(-k\ (x - x_0))}, \tag{5}$$

where x is the LocalPSNR value, x_0 is the midpoint of LocalPSNR value, and k is the logistic growth rate. The fitting curve is plotted as the solid line in Fig. 11(d). From the fitting curve, we assume the perception limit is the local PSNR value whose indistinguishable rate is 0.9. Above this perception limit, only less than 10% of the observers can perceive the difference between the rendered and target images. Similar curve fitting processes can be done for other images or on different ambient light conditions. Therefore, various perception limits are derived, based on the image contents and ambient light conditions.

3.3. D-value verification

From our subjective experiments, the perceptual limits of various images are different. For the images with low perceptual limits, it is difficult for HVS to recognize halo artifacts. Therefore, even if there is still a large image difference between the simulated image (mLCD) and the control image (OLED display), the observers cannot distinguish the halo artifacts. On the other hand, in some images, the perceptual limit is high. In this case, in order to avoid the notorious halo effect, it is necessary to increase the number of local dimming zones or the LCD's native contrast ratio. Therefore, the statistical perception limit from subjective experiments can also be regarded as the standard for evaluating the difficulty of halo effect detected by HVS. As a result, this visual experimental result is used to verify the numerical D-value method proposed above. If we depict the perceptual limit based on subjective experiments (20 different images are composed of 5 images under 4 different environmental conditions) as a function of the calculated D-value, the obvious positive correlation is shown in Fig. 12. Therefore, through subjective experiments, our newly proposed D-value function is proven to have the ability to reflect the difficulty of HVS to detect the halo effect under different image contents.

In practical applications, once the D-value of the target image is calculated, the perceptual limit of the target image can be found through the fitting curve between perceptual limit and D value as Fig. 12 shows. After that, using the evaluation metric LocalPSNR, the required number of local dimming zones for an mLCD with indistinguishable halo effects can be obtained. In all processes, the complicated subjective experiments are no longer required.

3.4. Different ambient environment

Four types of ambient condition are taken into consideration in our subjective experimental results, the required zones number of mLCD to eliminate the halo artifacts is shown in the Fig. 13. In most images shown in Figs. 13(a), 13(b), and 13(d), as the ambient light increases, the halo artifacts are washed out and thereby fewer zone number can achieve same image quality. However, in Fig. 13(e), the D-value of this image is the largest among all the five images evaluated: the D-value for Parking sign is 50.05, Ferris wheel is 8.63, Mountains is 2.33, Chess is 34.44, and

Optics EXPRESS

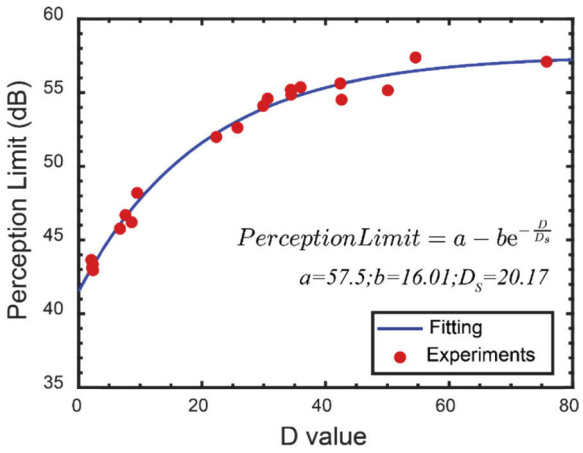

Fig. 12. The fitting curve of perception limit (human vision test) vs. D value (numerical calculation).

Tower is 75.78. As mentioned above, a large D-value indicates that the halo effect in the image is easy to recognize by HVS. Thus, even if we increase the CR of the LCD panel or ambient light illuminance, the required local dimming zones number is still high. On the other hand, in Fig. 13(c), the D value of this image is the lowest among all test images so the halo effect in the image is hard to distinguish by HVS. The observers cannot see the halo artifacts even though the zone number is only 18. The benefit of making more local dimming zones is limited. In these two extreme cases, local dimming cannot provide great improvement in image quality.

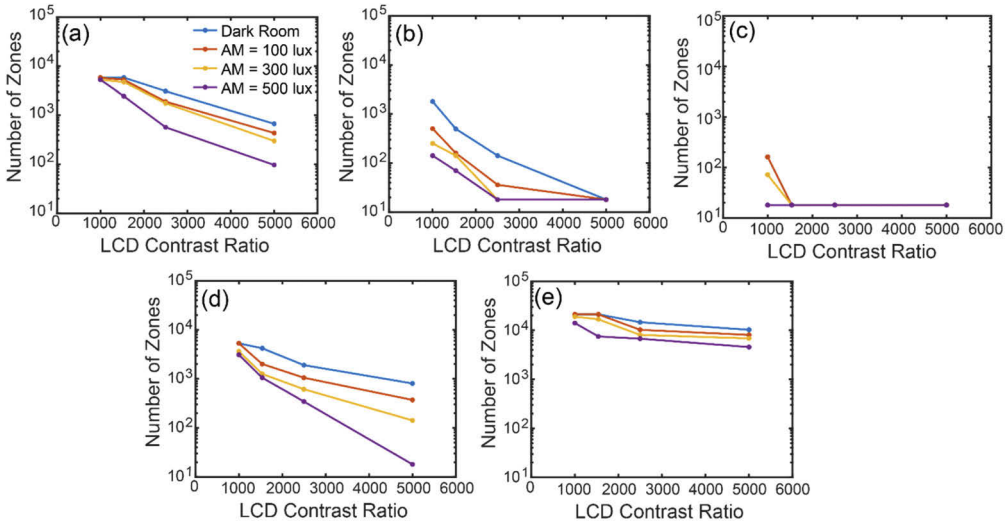

Fig. 13. Required local dimming zone number to suppress the halo effect under different ambient lighting: (a) Parking sign, (b) Ferris Wheel, (c) Mountains, (d) Chess, and (e) Tower.

In the following discussion, as we define a suitable local dimming zone number for different ambient light conditions, we focus on the images whose quality can be improved by the local dimming method. The average zone number from these images under different ambient conditions is shown in Fig. 14. According to our subjective experiment, as the ambient light gets brighter,

Optics EXPRESS

the halo effect is alleviated. Thus, an mLCD can obtain comparable image quality to OLED with a fewer local dimming zone number. In addition, the LCD panel with a high native contrast ratio leads to weak halo artifacts, which is easier to be washed out by the ambient light. For example, for an mLCD with CR=1000, the required zone number is reduced from 4500 to 2800 when the ambient light increases from 0 to 500 lux. However, in the same ambient light range, when the LCD's CR = 5000, the required zone number drops from 500 to 40.

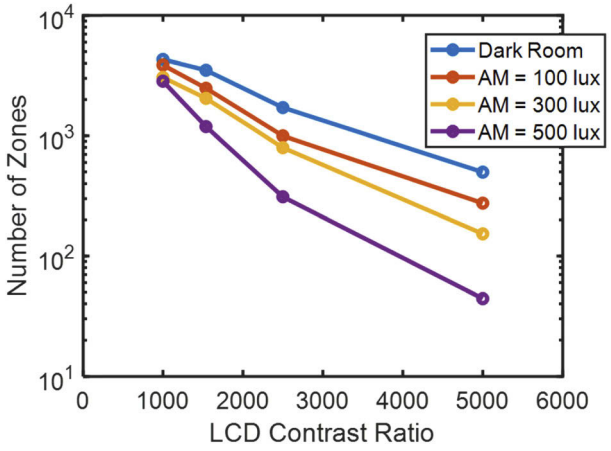

Fig. 14. Required local dimming zone number to achieve indistinguishable halo effect under different ambient lighting conditions. Here, we only consider those image contents that can be improved through local dimming

4. Discussion

As discussed above, the viewing angle in our visual experiments and simulations is at normal. However, as the panel size increases, the viewing angle for those pixels near the edges of the display increases. According to the statistical results (83 households), to cover entire display panel, the horizontal viewing angle is about ±40° [35]. Therefore, the halo effect of the mLCD under different viewing angles is also very important. Two popular LCD operating modes (MVA and FFS) are analyzed below. The higher on-axis contrast ratio (CR~5000:1) is the advantage of MVA LCD, while FFS mode provides a wider viewing angle and smaller gamma shift. As the viewing angle increases from 0 to 40°, the contrast ratio of MVA LCD decreases from ~5000:1 to ~2000:1, and the contrast ratio of FFS LCD decreases from ~2200:1 to ~1500:1 [8]. Figures 15(a) and 15(b) shows the number of required local dimming zones as a function of viewing angle for MVA and FFS LCDs, respectively. We can clearly see that as the viewing angle increases, the number of local dimming zones required for MVA LCD increases dramatically. However, such an increase for FFS LCD is very mild. Therefore, to suppress the halo effect to an indistinguishable level within ±40° of horizontal viewing angle, the number of local dimming zones required for FFS and MVA LCDs is similar (~3000 in dark zoom).

In the following, we explain why FFS LCD is a better choice for the mLCD system. 1) Dynamic contrast ratio. In the mLCD system, the dark state is not only determined by the LCD's native contrast ratio but also by the local dimming of the mini-LED backlight. With the support of local dimming methods, FFS LCD can also achieve a very high contrast ratio (CR $\geq 10^5$:1). The major advantage of MVA LCD of high on-axis contrast becomes less important. 2) Required zone number. As mentioned above, to maintain an indistinguishable level within ±40° viewing angle, the required local dimming zones in FFS and MVA LCDs is similar. 3) Gamma shift and color shift. Due to homogeneous alignment, FFS exhibits a much weaker gamma shift and

Optics EXPRESS

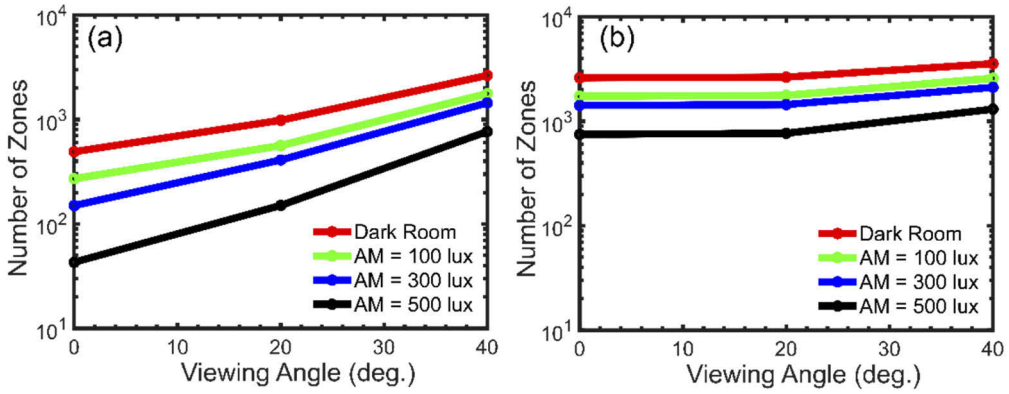

Fig. 15. Required number of local dimming zones for achieving indistinguishable halo effect under different viewing angle: (a) MVA LCD, and (b) FFS LCD.

color shift than MVA LCD [36]. Therefore, FFS LCD can maintain better image quality at a larger viewing angle. Moreover, FFS is more robust than MVA for touch panels. Based on these advantages, FFS LCD is a strong contender for the mLCD systems.

5. Conclusion

We have developed an optical simulation model to evaluate the influence of glare on the halo effect of HDR mLCDs. Based on the model, we further propose a D-value function to assess the difficulty of how human visual system distinguishes the halo effect. On one hand, it can find the local areas in an image with more severe halo effect. By calculating the PSNR in these local areas, a performance metric LocalPSNR is proposed to evaluate the image quality degraded by the halo effect. On the other hand, it can be used to evaluate the dependency between halo effect and image content. According to our results, if the D-value is too large (75.78) or too small (2.33), the image quality cannot be improved too noticeably by the local dimming method. Further visual experiment should be conducted to find a proper D-value range for evaluating all the image contents. In addition, we evaluate the required local dimming zones under different viewing angle and ambient light illuminance. As the ambient illuminance increases from 0 (dark room) to 500 lux, the dimming zones required to suppress the halo effect is reduced by ~10x. Through analyzing the dynamic contrast ratio, gamma shift and local dimming zone requirement for practical applications (300-lux ambient light and ±40° viewing angle, we find that FFS LCD is a strong contender for the mLCD system.

Funding

Nichia Corp.

Acknowledgments

The authors are indebted to Nichia Corp. for the financial support, and Hajime Akimoto, Taketoshi Nakano, and Nathan Wu for useful discussion.

Disclosures

The authors declare no conflicts of interest.

Optics EXPRESS

See Supplement 1 for supporting content.

References

1. H. Seetzen, W. Heidrich, W. Stuerzlinger, G. Ward, L. Whitehead, M. Trentacoste, A. Ghosh, and A. Vorozcovs, "High dynamic range display systems," ACM Trans. Graph. **23**(3), 760–768 (2004).
2. C. Chinnock, "Dolby Vision and HDR10," White Paper of Insight Media (2016).
3. S. Daly, T. Kunkel, X. Sun, S. Farrell, and P. Crum, "Viewer preferences for shadow, diffuse, specular, and emissive luminance limits of high dynamic range displays," SID Symp. Dig. Tech. Papers **44**(1), 563–566 (2013).
4. K. Masaoka and Y. Nishida, "Metric of color-space coverage for wide-gamut displays," Opt. Express **23**(6), 7802–7808 (2015).
5. J. L. Helman, "Invited paper: Delivering high dynamic range video to consumer devices," SID Symp. Dig. Tech. Papers **46**(1), 292–295 (2015).
6. Y. Huang, E. L. Hsiang, M. Y. Deng, and S. T. Wu, "Mini-LED, Micro-LED and OLED displays: Present status and future perspectives," Light: Sci. Appl. **9**(1), 105 (2020).
7. S. H. Lee, S. L. Lee, and H. Y. Kim, "Electro-optic characteristics and switching principle of a nematic liquid crystal cell controlled by fringe-field switching," Appl. Phys. Lett. **73**(20), 2881–2883 (1998).
8. H. Chen, G. Tan, M. C. Li, S. L. Lee, and S. T. Wu, "Depolarization effect in liquid crystal displays," Opt. Express **25**(10), 11315–11328 (2017).
9. S. Scholz, D. Kondakov, B. Lussem, and K. Leo, "Degradation mechanisms and reactions in organic light-emitting devices," Chem. Rev. **115**(16), 8449–8503 (2015).
10. H. Chen, J. Sung, T. Ha, and Y. Park, "Locally pixel-compensated backlight dimming on LED-backlit LCD TV," J. Soc. Inf. Disp. **15**(12), 981–988 (2007).
11. C. C. Lai and C. C. Tsai, "Backlight power reduction and image contrast enhancement using adaptive dimming for global backlight applications," IEEE Trans. Consumer Electron. **54**(2), 669–674 (2008).
12. H. G. Hulze and P. deGreef, "Power savings by local dimming on a LCD panel with side lit backlight," SID Symp. Dig. Tech. Papers **40**(1), 749–752 (2009).
13. T. Shirai, S. Shimizukawa, T. Shiga, S. Mikoshiba, and K. Käläntär, "RGB-LED backlights for LCD-TVs with 0D, 1D, and 2D adaptive dimming," SID Symp. Dig. Tech. Papers **37**(1), 1520–1523 (2006).
14. G. W. Yoon, S. W. Bae, Y. B. Lee, and J. B. Yoon, "Edge-lit LCD backlight unit for 2D local dimming," Opt. Express **26**(16), 20802–20812 (2018).
15. S. Cha, T. Choi, H. Lee, and S. Sull, "An optimized backlight local dimming algorithm for edge-lit LED backlight LCDs," J. Disp. Technol. **11**(4), 378–385 (2015).
16. T. Shiga and S. Mikoshiba, "Reduction of LCTV backlight power and enhancement of gray scale capability by using an adaptive dimming technique," SID Symp. Dig. Tech. Papers **34**(1), 1364–1367 (2003).
17. D. M. Hoffman, N. N. Stepien, and W. Xiong, "The importance of native panel contrast and local dimming density on perceived image quality of high dynamic range displays," J. Soc. Inf. Disp. **24**(4), 216–228 (2016).
18. Y. E. Wu, M. H. Lee, Y. C. Lin, C. Kuo, Y. H. Lin, and W. M. Huang, "Active Matrix Mini-LED Backlights for 1000PPI VR LCD," SID Symp. Dig. Tech. Papers **50**(1), 562–565 (2019).
19. B. Zheng, Z. Deng, J. Zheng, L. Wu, W. Yang, Z. Lin, H. Wang, P. Shen, and J. Li, "An Advanced High-Dynamic-Range LCD for Smartphones," SID Symp. Dig. Tech. Papers **50**(1), 566–568 (2019).
20. T. Masuda, H. Watanabe, Y. Kyoukane, H. Yasunaga, H. Miyata, M. Yashiki, T. Nara, and T. Ishida, "Mini-LED Backlight for HDR Compatible Mobile Displays," SID Symp. Dig. Tech. Papers **50**(1), 390–393 (2019).
21. H. Chen, T. H. Ha, J. H. Sung, H. R. Kim, and B. H. Han, "Evaluation of LCD local-dimming-backlight system," J. Soc. Inf. Disp. **18**(1), 57–65 (2010).
22. Y. Huang, G. Tan, F. Gou, M. C. Li, S. L. Lee, and S. T. Wu, "Prospects and challenges of mini-LED and micro-LED displays," J. Soc. Inf. Disp. **27**(7), 387–401 (2019).
23. S. Cha, T. Choi, H. Lee, and S. Sull, "An optimized backlight local dimming algorithm for edge-lit LED backlight LCDs," J. Soc. Inf. Disp. **11**(4), 378–385 (2015).
24. N. Burini, E. Nadernejad, J. Korhonen, S. Forchhammer, and X. Wu, "Modeling power-constrained optimal backlight dimming for color displays," J. Disp. Technol. **9**(8), 656–665 (2013).
25. S. J. Song, Y. I. Kim, J. Bae, and H. Nam, "Deep-learning-based pixel compensation algorithm for local dimming liquid crystal displays of quantum-dot backlights," Opt. Express **27**(11), 15907–15917 (2019).
26. S. K. Kim, S. J. Song, and H. Nam, "Bilinear weighting and threshold scheme for low-power two-dimensional local dimming liquid crystal displays without block artifacts," Opt. Eng. **53**(6), 063110 (2014).
27. G. Tan, Y. Huang, M. C. Li, S. L. Lee, and S. T. Wu, "High dynamic range liquid crystal displays with a mini-LED backlight," Opt. Express **26**(13), 16572–16584 (2018).
28. J. J. McCann and V. Vonikakis, "Calculating retinal contrast from scene content: a program," Front. Psychol. **8**, 2079 (2018).
29. J. J. McCann and A. Rizzi, "Camera and visual veiling glare in HDR images," J. Soc. Inf. Disp. **15**(9), 721–730 (2007).
30. J. J. Vos and T. J. T. P. van den Berg, "Report on Disability Glare," CIE Collection **135**, 1–9 (1999).

Optics EXPRESS

31. J. Korhonen, N. Burini, S. Forchhammer, and J. M. Pedersen, "Modeling LCD displays with local backlight dimming for image quality assessment," Proc. SPIE **7866**, 786607 (2011).
32. P. G. J. Barten, *Contrast sensitivity of the human eye and its effects on image quality*. (SPIE, 1999).
33. H. Strasburger, I. Rentschler, and M. Jüttner, "Peripheral vision and pattern recognition: A review," J Vis. **11**(5), 13 (2011).
34. J. H. Lee, X. Zhu, Y. H. Lin, W. K. Choi, T. C. Lin, S. C. Hsu, H. Y. Lin, and S. T. Wu, "High ambient-contrast-ratio display using tandem reflective liquid crystal display and organic light-emitting device," Opt. Express **13**(23), 9431–9438 (2005).
35. Y. Igarashi, S. Kubota, M. Takemoto, K. Kishimoto, K. Inoguchi, Y. Yamamoto, T. Matsumoto, S. Haga, and T. Nakatsue, "Investigation on Viewing Angle Requirements and Glare with Respect to Size of Flat-panel Television Displays," SID Symp. Digest Tech. Papers **43**(1), 820–823 (2012).
36. R. Lu, X. Nie, and S. T. Wu, "Color performance of an MVA-LCD using an LED backlight," J. Soc. Inf. Disp. **16**(11), 1139–1145 (2008).